Journal Name

ARTICLE TYPE

Cite this: DOI: 10.1039/xxxxxxxxxx

A Maxwell Relation for Dynamical Timescales with Application to the Pressure and Temperature Dependence of Water Self-Diffusion and Shear Viscosity†

Zeke A. Piskulich,[a,b] Ashley K. Borkowski,[a] and Ward H. Thompson[a*]

Received Date
Accepted Date

DOI: 10.1039/xxxxxxxxxx

www.rsc.org/journalname

A Maxwell relation for a reaction rate constant (or other dynamical timescale) obtained under constant pressure, p, and temperature, T, is introduced and discussed. Examination of this relationship in the context of fluctuation theory provides insight into the p and T dependence of the timescale and the underlying molecular origins. This Maxwell relation motivates a suggestion for the general form of the timescale as a function of pressure and temperature. This is illustrated by accurately fitting simulation results and existing experimental data on the self-diffusion coefficient and shear viscosity of liquid water. A key advantage of this approach is that each fitting parameter is physically meaningful.

1 Introduction

Practically every undergraduate physical chemistry student learns about the Maxwell relations that provide important connections between thermodynamic variables.[1] These relationships arise naturally from the fact that thermodynamic functions such as enthalpy and free energy are state functions. Further, they are used to provide a deeper understanding of the properties of chemical systems, *e.g.*, how entropy changes with volume at constant temperature.[1]

In examining chemical dynamics, one often faces the same issue that motivates the Maxwell relations: How does a property change with the independent thermodynamic variables like pressure (p) and temperature (T)? The difference is that the fundamental quantities of interest are dynamical, *e.g.*, reaction rate constants, timescales, or transport coefficients. Indeed, the temperature dependence of a reaction rate constant, expressed as the activation energy, is a central feature of reaction rate theory.[2–4] Similarly, while significantly less attention has been paid to it, the activation volume characterizes the change of a rate constant with pressure.[5,6]

In the Arrhenius perspective, the activation energy is assumed to be constant and provides insight into the magnitude of the (fixed) underlying energetic barrier of the process.[1,4] However, for some processes non-Arrhenius behavior is quantitatively and qualitatively important. The dynamics of liquid water is one such case, where temperature-dependent activation energies have been observed for diffusion,[7–11,11–16] reorientation dynamics,[12,14,16,17] and viscosity;[14,18–21] these processes have a common underlying barrier associated with the exchange of hydrogen-bond (H-bond) acceptors,[22] which itself exhibits non-Arrhenius behavior that are largely attributed to changes in the H-bond network. Other cases are enzymatic reactions[23] and reactions in which quantum mechanical tunneling represents a significant contribution (typically at lower temperatures).[24]

The effect of pressure on dynamical processes is typically much more modest than that of temperature and can often only be resolved by varying p by tens or hundreds of MPa.[25–29] In many cases, this behavior is Arrhenius-like, *i.e.*, the activation volume is constant with pressure. Then, the activation volume can be obtained from an Arrhenius analysis based on measurement or simulation of the rate constant, or other dynamical timescale, at a few (widely different) pressures. In other systems, however, the activation volume can change significantly, even in the sign, as the pressure is varied. Because the activation volume represents the relative space taken up by the transition state configuration compared to that of the reactants, this suggests a change in the mechanistic details. Note that the "volume" difference here applies to the entire system, including any arrangements of the solvent, whether it is innocent in the reaction or not.[30]

In cases where the activation energy is not constant with thermodynamic conditions, a full understanding of the dynamics requires a description of how the energy required to carry out the process of interest changes with the temperature and pressure. The same is certainly true of the activation volume. In this Paper we explore this issue theoretically, in the context of an effective Maxwell relation for dynamical timescales. Based on this relation, we propose a method for global fitting of a dynamical

[a] *Department of Chemistry, University of Kansas, Lawrence, KS 66045, USA. E-mail: wthompson@ku.edu*
[b] *Current Address: Department of Chemistry, Boston University, Boston, MA, 02215, USA.*

timescale based on these ideas that is parameterized only by physically meaningful quantities and demonstrate it by analysis of the extensive existing experimental data for the water diffusion coefficient and shear viscosity as well as simulation results for the former.

2 Theory

2.1 Maxwell Relation for a Dynamical Variable

In the isothermal-isobaric (NpT) ensemble, we can consider a generic rate constant, transport coefficient, or (inverse) timescale – which we will denote as k – as a function of the independent thermodynamic variables, for fixed N, such that its total differential is given by

$$dk = \left(\frac{\partial k}{\partial T}\right)_{p,N} dT + \left(\frac{\partial k}{\partial p}\right)_{T,N} dp. \tag{1}$$

It will be convenient to consider $\ln k$ rather than the rate constant itself and to use $\beta = 1/k_B T$ instead of T as an independent variable (where k_B is Boltzmann's constant). Then, we have

$$d(\ln k) = \left(\frac{\partial \ln k}{\partial \beta}\right)_p d\beta + \left(\frac{\partial \ln k}{\partial p}\right)_\beta dp, \tag{2}$$

as the total differential of interest.

The partial derivatives appearing in eqn (2) can be identified as physically meaningful, measurable quantities in reaction rate theory (and in the theory of transport coefficients). Namely, the activation energy, E_a, is given by the first derivative with respect to β:

$$\left(\frac{\partial \ln k}{\partial \beta}\right)_p = -E_a, \tag{3}$$

i.e., a measure of the temperature dependence of k. Similarly,

$$\left(\frac{\partial \ln k}{\partial p}\right)_\beta = -\beta \Delta V^\ddagger, \tag{4}$$

gives the activation volume, $\Delta V^\ddagger$, reflecting how k is influenced by pressure. Thus, the total differential of k, can be written as

$$d(\ln k) = -E_a d\beta - \beta \Delta V^\ddagger dp, \tag{5}$$

which suggests that we can think of β and p as natural variables of the rate constant (or transport coefficient).

We can then proceed in complete analogy to the derivation of a thermodynamic Maxwell relation, by noting that the rate constant k is a state function and thus,

$$\left(\frac{\partial^2 \ln k}{\partial p \partial \beta}\right) = \left(\frac{\partial^2 \ln k}{\partial \beta \partial p}\right). \tag{6}$$

Evaluating these cross-derivatives yields the Maxwell relation

$$\left(\frac{\partial E_a}{\partial p}\right)_\beta = \Delta V^\ddagger + \beta \left(\frac{\partial \Delta V^\ddagger}{\partial \beta}\right)_p. \tag{7}$$

This equation demonstrates the relationship between the pressure dependence of the activation energy to the temperature dependence of the activation volume. Because the meaning of k is general, this equation should hold for rate constants, transport coefficients, and other dynamical timescales. Such Maxwell relationships for dynamical activation barriers have not been much explored, but, as we discuss here, they can prove useful and important. We note that previously Kelm and Palmer argued that an analogous Maxwell relation should exist for the activation enthalpy and volume defined with transition state theory,[31] and Brauer and Kelm verified, through measurements on the Menshutkin reaction, the validity of the relation.[32] In the following, we examine the underpinnings of this Maxwell relation.

2.2 Fluctuation Theory and the Maxwell Relation

It is instructive to examine how the Maxwell relation in eqn (7) arises naturally within fluctuation theory. We can consider an ensemble of NpT trajectories, each with a different (fixed) energy and volume, such that the rate constant is given by

$$k = \langle k_i \rangle = \frac{1}{\Omega(N,p,T)} \mathrm{Tr}\left[e^{-\beta(U_i + pV_i)} k_i\right], \tag{8}$$

where U_i and V_i are the fixed internal energy and volume of the i^{th} trajectory and Tr indicates a sum over all the trajectories, $\Omega(N,p,T) = \mathrm{Tr}[e^{-\beta(U_i+pV_i)}]$ is the isothermal-isobaric partition function, and thus $\langle \cdots \rangle$, indicates an ensemble average. Note that k_i is itself an average over the i^{th} constant energy and volume trajectory, typically a time correlation function, *e.g.*, for a reaction rate constant $\lim_{t\to\mathrm{long}} \langle F_s(0)\, \theta[s(t)] \rangle_i$ where F_s is the flux across the transition state dividing surface defined by $s = 0$ and θ is the Heaviside step function. Recall, however, that k can also be a transport coefficient or other dynamical quantity, which are also expressible as averaged time correlation functions.

We have earlier shown[33–35] that the derivatives of eqn (8) with respect to the independent thermodynamic variables can be expressed in terms of fluctuations. Namely, it is straightforward to show that

$$\frac{\partial k}{\partial \beta} = -\langle [\delta U_i + p \delta V_i]\, k_i \rangle, \tag{9}$$

where $\delta U_i = U_i - \langle U_i \rangle$ and $\delta V_i = V_i - \langle V_i \rangle$ are the fluctuations in energy and volume respectively of the i^{th} trajectory from the average of all the (constant volume and energy) trajectories that are prepared in the NpT ensemble. Similarly, the pressure derivative is given by

$$\frac{\partial k}{\partial p} = -\beta \langle \delta V_i k_i \rangle. \tag{10}$$

Both of these quantities can be directly calculated from an ensemble of isothermal-isobaric trajectories at a single temperature and pressure;[12,34,35] see Sec. 3.

The activation energy can be obtained by combining eqns (9) and (3) to yield

$$E_a = \frac{\langle [\delta U_i + p \delta V_i]\, k_i \rangle}{\langle k_i \rangle}. \tag{11}$$

This fluctuation theory result has a straightfoward and useful physical interpretation. The activation energy is the correlation of the enthalpy of the system, $H_i = U_i + pV_i$ with the rate constant. Thus, if, when the enthalpy is larger (smaller) than average the process is faster (slower), E_a is positive. The greater the effect of an enthalpy fluctuation on the rate constant, the larger the mag-

nitude of the activation energy. This activation energy includes, as one component, the activation volume. This can be seen by using eqns (10) and (4), to find

$$\Delta V^{\ddagger} = \frac{\langle \delta V_i k_i \rangle}{\langle k_i \rangle}. \tag{12}$$

This is the first term on the right-hand-side (*rhs*) of the Maxwell relation, eqn (7). It also has an analogous interpretation to the activation energy in that it measures the effect of the volume on the rate constant.

The remaining terms in the Maxwell relation are more challenging to interpret as they involve higher, cross derivatives. However, the second term on the *rhs* of eqn (7) can be obtained by taking the derivative of eqn (12) with respect to β. This gives

$$\frac{\partial \Delta V^{\ddagger}}{\partial \beta} = \frac{1}{\langle k_i \rangle} \frac{\partial \langle \delta V_i k_i \rangle}{\partial \beta} + \Delta V^{\ddagger} E_a. \tag{13}$$

The derivative in the first term is more explicitly written as

$$\frac{\partial \langle \delta V_i k_i \rangle}{\partial \beta} = \frac{\partial}{\partial \beta} \frac{1}{\Omega(N,p,T)} \mathrm{Tr}\left[e^{-\beta(U_i + pV_i)} \delta V_i k_i \right], \tag{14}$$

which involves three terms due to the temperature dependence of $\Omega(N,p,T)$, the Boltzmann factor, and the average volume appearing in δV_i. Evaluating the derivative yields

$$\begin{aligned} \frac{\partial \langle \delta V_i k_i \rangle}{\partial \beta} &= \langle U_i + pV_i \rangle \langle \delta V_i k_i \rangle - \langle [U_i + pV_i] \delta V_i k_i \rangle \\ &- \frac{\partial \langle V_i \rangle}{\partial \beta} \langle k_i \rangle \\ &= -\langle [\delta U_i + p \delta V_i] \delta V_i k_i \rangle - \frac{\partial \langle V_i \rangle}{\partial \beta} \langle k_i \rangle. \end{aligned} \tag{15}$$

Thus, we find

$$\begin{aligned} \beta \frac{\partial \Delta V^{\ddagger}}{\partial \beta} &= -\beta \frac{\langle [\delta U_i + p \delta V_i] \delta V_i k_i \rangle}{\langle k_i \rangle} \\ &- \beta \frac{\partial \langle V_i \rangle}{\partial \beta} + \beta \Delta V^{\ddagger} E_a, \end{aligned} \tag{16}$$

is the second term on the *rhs* of the Maxwell relation.

The left-hand-side (*lhs*) of eqn (7) can be derived in a completely analogous fashion. From eqns (11) and (10), we have

$$\frac{\partial E_a}{\partial p} = \frac{1}{\langle k_i \rangle} \frac{\partial \langle [\delta U_i + p \delta V_i] k_i \rangle}{\partial p} + E_a \beta \Delta V^{\ddagger}. \tag{17}$$

The first term has three pressure-dependent quantities and proceeding as before, it is straightfoward to show that

$$\begin{aligned} \frac{\partial E_a}{\partial p} &= -\beta \frac{\langle [\delta U_i + p \delta V_i] \delta V_i k_i \rangle}{\langle k_i \rangle} + \Delta V^{\ddagger} \\ &+ \beta \Delta V^{\ddagger} E_a - \frac{\partial \langle U_i \rangle}{\partial p} - p \frac{\partial \langle V_i \rangle}{\partial p}, \end{aligned} \tag{18}$$

represents the *lhs* of the Maxwell relation in eqn (7).

Comparing the fluctuation theory results for the *lhs* and *rhs* of the Maxwell relation using eqns (18) and (16), it is clear that it holds if

$$\frac{\partial \langle U_i \rangle}{\partial p} + p \frac{\partial \langle V_i \rangle}{\partial p} = \beta \frac{\partial \langle V_i \rangle}{\partial \beta}. \tag{19}$$

This equation does not involve any dynamical property and is a purely thermodynamic relationship that involves the averages present in the fluctuations. It is not hard to show that it is equivalent to the connection, derived using a thermodynamic Maxwell relation, between the pressure derivative of the enthalpy, $H = \langle U_i + pV_i \rangle$, and the temperature derivative of the volume

$$\left(\frac{\partial H}{\partial p} \right)_T = T \left(\frac{dS}{dp} \right)_T + V = \beta \left(\frac{dV}{d\beta} \right)_p + V, \tag{20}$$

where S is the entropy.

Thus, we have evaluated the Maxwell relation for a dynamical quantity, eqn (7), within the context of fluctuation theory. A key result is that the central quantity is the second-order correlation of the fluctuations,

$$-\beta \frac{\langle [\delta U_i + p \delta V_i] \delta V_i k_i \rangle}{\langle k_i \rangle}, \tag{21}$$

that describes both the pressure dependence of the activation energy and the temperature dependence of the activation volume. This illustrates the microscopic origin of the Maxwell relation as the cross-correlation of the enthalpy *and* volume fluctuations with the dynamics. While not the focus of the present work, we have previously shown how similar quantities can be calculated from MD simulations, *e.g.*, E_a, $\Delta V^{\ddagger}$, and $\partial E_a / \partial \beta$,[12,36] and the same should be true of eqn (21).

In Sec. 4 we consider this Maxwell relation in the context of liquid water self-diffusion and viscosity. It is known that water diffusion exhibits an interesting temperature dependence of $\Delta V^{\ddagger}$ (and consequently pressure dependence of E_a)[7–13,34,37–39] The generality of the equations shown above for a nominal rate constant k are straightforwardly applied to the case of the water diffusion coefficient and viscosity.

3 Computational Methods

We have calculated the water self-diffusion coefficient at a range of temperatures and pressures using molecular dynamics simulations of 343 TIP4P/2005[40] water molecules. The simulations were carried out with the LAMMPS code.[41] For each p and T a 10 ns NpT trajectory was propagated using a three-chain Nosé-Hoover thermostat and barostat.[42,43] A simulation timestep of 1 fs was used, and the thermostat and barostat damping parameters were 100 fs and 1 ps, respectively. The molecules were held rigid using the SHAKE algorithm with a 1.0×10^{-4} tolerance parameter. The Particle-Particle-Particle-Mesh (PPPM) method[44,45] was used to calculate long-range electrostatic interactions (tolerance parameter of 1.0×10^{-4}). Tail corrections were included to achieve the correct density. From each simulation, 10,000 configurations, each separated by 1 ps, were used as starting points for 20 ps NVE trajectories. From each NVE trajectory, the mean-squared-displacement, $MSD(t) = \langle |\vec{r}(t) - \vec{r}(0)|^2 \rangle$, was calculated for $t = 0$ to 20 ps with multiple time origins separated by 1 ps, the last 10 ps of which was fit to a line to compute $D_i = \mathrm{slope}_i / 6$.

All uncertainties were calculated over 10 blocks (each of 1,000 trajectories) and represent a 95% confidence interval based on the Student's t-distribution.[46]

4 Results and Discussion

The Maxwell relation given in eqn (7) and its origins suggest a way to describe the pressure and temperature dependence of a dynamical quantity in a physically motivated way. Here, we explore this approach for the particular case of the water self-diffusion coefficient, D, and shear viscosity, η, but it is completely general and could be equally well applied to reaction rate constants or dynamical timescales, as long as they are measures of activated processes.

4.1 Water Self-Diffusion

The water diffusion coefficient (like other dynamical properties of liquid water) is well-known to be significantly non-Arrhenius.[7–13] We can describe this behavior by a second-order Taylor series expansion in p and β about a set of reference values,

$$\begin{aligned}\ln D(p,\beta) &= \ln D(p_0,\beta_0) + \left.\frac{\partial \ln D}{\partial \beta}\right|_0 (\beta-\beta_0) \\ &+ \left.\frac{\partial \ln D}{\partial p}\right|_0 (p-p_0) + \frac{1}{2}\left.\frac{\partial^2 \ln D}{\partial \beta^2}\right|_0 (\beta-\beta_0)^2 \\ &+ \frac{1}{2}\left.\frac{\partial^2 \ln D}{\partial p^2}\right|_0 (p-p_0)^2 \\ &+ \left.\frac{\partial^2 \ln D}{\partial p \partial \beta}\right|_0 (p-p_0)(\beta-\beta_0), \end{aligned} \quad (22)$$

where the subscript "0" on the derivatives indicates evaluation at the reference point, p_0 and β_0. However, we can identify the derivatives of $\ln D$ as the activation energy and volume so that this can be written as,

$$\begin{aligned}\ln \frac{D(p,\beta)}{D(p_0,\beta_0)} &= -E_{a,0}\Delta\beta - \beta_0 \Delta V_0^{\ddagger}\Delta p - \frac{1}{2}\left.\frac{\partial E_a}{\partial \beta}\right|_0 \Delta\beta^2 \\ &- \frac{\beta_0}{2}\left.\frac{\partial \Delta V^{\ddagger}}{\partial p}\right|_0 \Delta p^2 - \left.\frac{\partial E_a}{\partial p}\right|_0 \Delta p \Delta\beta, \end{aligned} \quad (23)$$

with $\Delta\beta = \beta - \beta_0$ and $\Delta p = p - p_0$. Here, we have noted that, in this explicitly non-Arrhenius description, the activation energy and volume are functions of p and β so that $E_{a,0}$ and $\Delta V_0^{\ddagger}$ indicate their values at p_0 and β_0. This approach follows and extends prior work involving low-order expansions of the activation energy in temperature[47,48] and the activation volume in pressure.[31] There is some evidence, however, that at very high pressures a second-order expansion may not suffice.[49]

Note that the Maxwell relation, eqn (7) can be used to express the last term in eqn (23), which, after some rearrangement, gives

$$\begin{aligned}\ln \frac{D(p,\beta)}{D(p_0,\beta_0)} &= -E_{a,0}\Delta\beta - \beta\Delta V_0^{\ddagger}\Delta p \\ &- \frac{1}{2}\left.\frac{\partial E_a}{\partial \beta}\right|_0 \Delta\beta^2 - \frac{\beta_0}{2}\left.\frac{\partial \Delta V^{\ddagger}}{\partial p}\right|_0 \Delta p^2 \\ &- \beta_0 \left.\frac{\partial \Delta V^{\ddagger}}{\partial \beta}\right|_0 \Delta p \Delta\beta. \end{aligned} \quad (24)$$

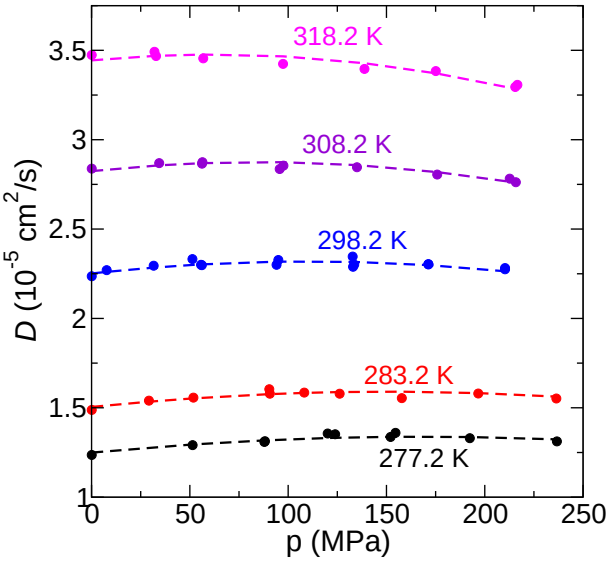

Fig. 1 Comparison of measured $D(p,T)$ (circles) from Woolf (Ref. 7) compared to its fit (dashed lines) to eqn (24).

Either of these two equivalent formulas, eqns (23) and (24), can be used to fit experimental measurements of the diffusion coefficient as a function of temperature and pressure. A key advantage of these expressions is that the fitting parameters represent physically meaningful properties: The activation energy, activation volume, and their first derivatives with respect to β and pressure, which represent the clearest measures of non-Arrhenius behavior.

While we will show that this is an excellent description of the diffusion coefficient over a wide pressure and temperature range, it would not be expected to describe the behavior of deeply supercooled water, *i.e.*, as the Widom line is approached.[50,51] Alternative formulations of $D(p,\beta)$ that explicitly incorporate the two liquids behavior[52] and the dynamical Maxwell relation are, however, possible.

We can illustrate and test the global description of the pressure and temperature dependence of the water diffusion coefficient by using eqn (24), or its equivalent eqn (23), to fit existing measurement data in the literature.[7–11] We consider results from five separate studies that have examined $D(p,T)$ for H_2O using NMR and diaphragm cell measurements over different ranges of pressure and temperature.

We first consider the measurements by Woolf of THO diffusion in H_2O using the diaphragm cell method;[7] note that these results

Table 1 Summary of nonlinear least-squared fits of eqn (24) to experimental measurements of the water self-diffusion coefficient as a function of p and T,[7–11] the present simulations, and direct fluctuation theory simulation results for TIP4P/2005 water.[36] Except for the direct calculations, each quantity in the table, including D, is determined from the fit with $\partial E_a/\partial p$ obtained from eqn (7). Values are for $T_0 = 298.15$ K and $p_0 = 0.1$ MPa for which $D = 2.299 \times 10^{-5}$ cm^2/s is the accepted experimental value.[13,53]

Quantity	Woolf[7a]	Krynicki *et al.*[8]	Harris *et al.*[9,10]	Prielmeier *et al.*[11b]	TIP4P/2005 Fit[c]	TIP4P/2005 Direct[d]	Units
D	2.24	2.23	2.29	2.20	2.02	2.37 ± 0.01	10^{-5} cm^2/s
E_a	17.96	18.43	17.49	17.13	17.00	17.15 ± 0.21	kJ/mol
$\Delta V^\ddagger$	-1.32	-0.14	-1.09	-2.25	-1.21	-1.19 ± 0.13	cm^3/mol
$\frac{\partial E_a}{\partial \beta}$	90.65	36.16	63.39	111.93	48.26		(kJ/mol)^2
$\frac{\partial \Delta V^\ddagger}{\partial p}$	1.18	0.83	1.01	1.82	0.69		10^{-2} cm^3/(mol MPa)
$\frac{\partial E_a}{\partial p}$	-9.43	-5.53	-5.02	-9.19	-9.75		cm^3/mol
$\beta \frac{\partial \Delta V^\ddagger}{\partial \beta}$	-8.12	-5.39	-3.93	-6.94	-8.54		cm^3/mol
RMSE	0.018	0.25	0.030	0.018	0.017		10^{-5} cm^2/s
χ^2	1.07	0.60[e]	1.14[f]	0.88[g]	1.86[h]		
Avg. Fit Error	0.69	2.30	0.89	2.10	0.61		%
Max. Fit Error	2.37	7.42	3.44	6.75	3.41		%

[a] Results are for THO in H_2O.
[b] Only results for $T \geq 252$ K were considered.
[c] These simulation results do not include corrections for finite-size effects,[54,55] which would give a larger value of $D = 2.36 \times 10^{-5}$ cm^2/s at 298.15 K and 0.1 MPa.[36]
[d] Direct calculations at 298.15 K and 0.1 MPa using fluctuation theory.[36]
[e] Assumes 5% error for all data points.[8]
[f] Assumes 1% error for all data points.[56]
[g] Assumes 3% error for all data points.[11]
[h] Errors used in calculation of χ^2 are 95% confidence intervals.

may exhibit some isotope effect compared to neat water. Temperatures from 277 to 318 K and pressures from 0.1 to ~ 240 MPa were considered and the results are shown in Fig. 1 and compared to the fit to eqn (24). The resulting fitting parameters are given in Table 1 and will be discussed below; note that six of the parameters are unique while $\partial E_a/\partial p$ and $\beta(\partial \Delta V^\ddagger/\partial \beta)$ are related through eqn (7). Woolf fit the diffusion data to an eight-parameter expression that has the characteristics of a polynomial in $1/T$ and obtained a root-mean-squared error (RMSE) from the data of 0.014×10^{-5} cm^2/s. The present fitting approach gives a comparable RMSE of 0.018×10^{-5} cm^2/s with two fewer parameters. Overall, Fig. 1 shows that eqn (24) does an excellent job of describing the experimental data with an even representation of the data at all p and T.

One of the largest data sets for water diffusion was provided by Krynicki *et al.* based on proton spin echo NMR measurements.[8] These data extend from 0.1 to 170 MPa and 275 to 498 K and are plotted in Fig. 2 where they are compared to their fit to eqn (24). In this case, the fit is not as good as that in Fig. 1, with the most marked deviations occurring in the 298.2 and 472.2 K isotherms. In particular, the fit underestimates D at room temperature for all pressures and also at 323.2 K for pressures above ~ 40 MPa. At 472.2 K the fit underestimates the rate of decrease of D with increasing pressure. There is reason to believe that the data of Krynicki *et al.* suffers from issues associated with the method of calibration used (see, *e.g.*, Ref. 10) that may make it less reliable than the other experimental studies considered here. We note that, in particular, the activation volume and its pressure derivative are lower than that obtained from the other data sets. Setting these deficiencies aside, however, the fit agreement is good for most of the temperatures and pressures explored; the average absolute error is 2.3%, on the same order of the error estimates of the measurements of 1.5-4%. Krynicki *et al.* fit their data with an empirical, six-parameter formula that appears to have comparable accuracy to the present fit.

Harris and Woolf reported measurements of D for 277-333 K and for pressures up to 300 MPa.[9] Using the same instrument, Harris and Newitt measured the diffusion coefficient at T below room temperature extending to pressures around 350 MPa.[10] Given their common origin, we have combined these data into a single set for fitting. It is worth noting that they observed some significant differences with the measurements of Krynicki *et al.*,[8] the primary one being that the latter observed the maximum in D with increasing p at lower pressures than Harris and Woolf (see Fig. 2 of Ref. 9). The data from Refs. 9 and 10 are presented in Fig. 3 and compared to the result of fitting to eqn (24). The fit is in excellent agreement with the measured D across the range of pressures and temperatures, even down to the lowest temper-

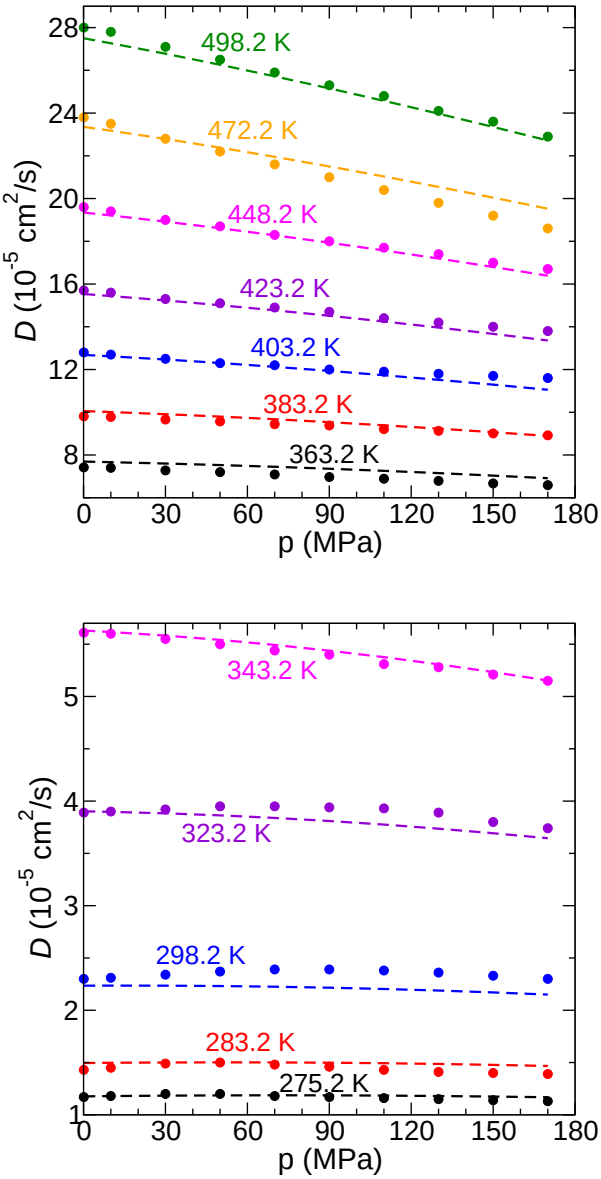

Fig. 2 Comparison of measured $D(p,T)$ (circles) from Krynicki, Green, and Sawyer (Ref. 8) compared to its fit (dashed lines) to eqn (24) at high (top panel) and low (bottom panel) temperatures.

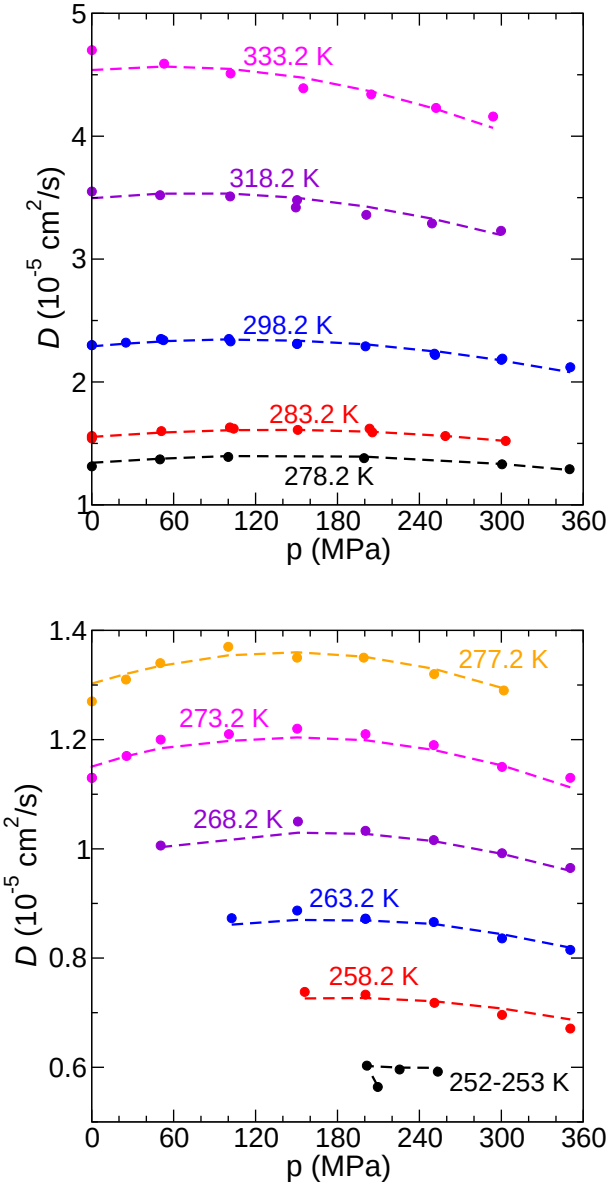

Fig. 3 Comparison of measured $D(p,T)$ (circles) from the Harris and Woolf (Ref. 9) and Harris and Newitt (Ref. 10) compared to the fit of the combined data sets (dashed lines) to eqn (24) at high (top panel) and low (bottom panel) temperatures. (Note the single point at 252 K is grouped with the data at 253 K to show its fit.)

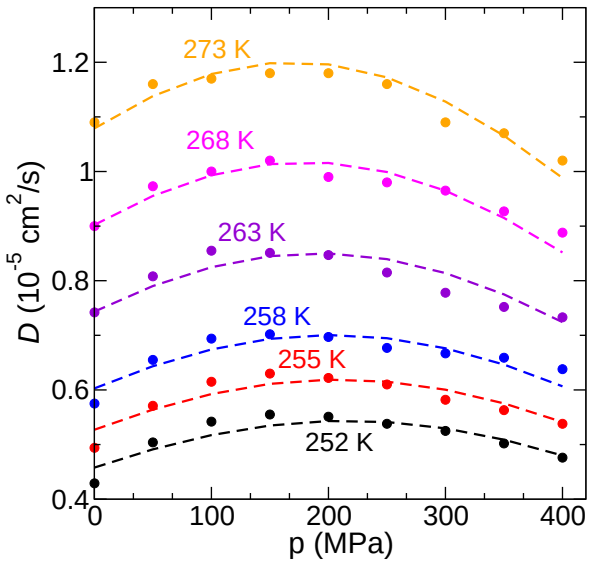

Fig. 4 Comparison of measured $D(p,T)$ (circles) from Prielmeier *et al.* (Ref. 11) compared to its proposed fit (dashed lines) to eqn (24).

ature of 252 K, with an average absolute error of $< 1\%$ and a maximum error of $< 3.5\%$. Harris and Woolf fit their data with the same eight-parameter empirical function used in Ref. 7 and obtained a RMSE of 0.016×10^{-5} cm^2/s, essentially of the same quality as we find if we fit that data alone.

Next, we turn to the fitting of the results of Prielmeier *et al.*,[11] who measured the diffusion coefficient for deeply supercooled water down to 203.5 K. We find that the fit quality is very good for the data where $T \geq 252$ K (see Table 1), but begins to degrade when data below 252 K are included. For the higher temperatures, we obtain a similar or smaller RMSE to the other three data sets with an average fit error of 2.10%.

It is important to note that the expansion in eqn (23) or (24) is based on an assumption of a relatively smooth variation of D with pressure and temperature. It is thus not expected that it would accurately describe the dramatic slowdown in the diffusion coefficient upon lowering the temperature toward the Widom line that lies at or below ~ 230 K.[50–52] It is therefore all the more encouraging that the approach works satisfactorily down to such low T for the data sets from Refs. 9 - 11. The behavior of water in the deeply supercooled regime that lies at even lower T has been a subject of intense interest with considerable evidence supporting a smooth, "two liquids," transition from a high-density liquid (HDL) to a low-density liquid (LDL) at the Widom line (the extension of the liquid-liquid coexistence curve beyond its terminal critical point[57,58]).[17,50–52,59] We anticipate that the fitting approach described here, which does not account for this effect, will not be adequate at significantly lower temperatures, and this indeed appears to be the case when considering the data of Prielmeier *et al.*.[11] However, the two-liquids perspective points to a natural extension,[12,17,51,59] where one writes $D(p,T) = s(p,T)\ln D_{LDL}(p,T) + [1 - s(p,T)]\ln D_{HDL}(p,T)$ with D_{LDL} and D_{HDL} described analogously to eqn (24); here, $s(T)$ is a switching function that goes smoothly from zero at low T to one at high T. This is an interesting avenue for future investigations.

We now turn to an examination of the results of the fitting, namely, the optimized parameters obtained for each data set that are provided in Table 1. All the fits naturally give values of D(0.1 MPa, 298.15 K) that are the same or close to the actual measured value. More interesting is the activation energy, for which values between 17.13-18.43 kJ/mol are obtained. These are close to the values of $E_a = 18.28$ and 18.11 kJ/mol found directly by Arrhenius analyses in Refs. 7 and 8, respectively. The results are also in good agreement with recent simulations using the TIP4P/2005 model[36] that are also provided in Table 1. There is considerably greater spread in the values obtained for the activation volume. All of the fits give $\Delta V^{\ddagger} < 0$, as do simulations,[36] but with magnitudes that vary from -0.14 to -2.25 cm^3/mol.

The other fitting parameters represent higher derivatives of the diffusion coefficient with respect to β and p. The non-Arrhenius behavior is most directly expressed in $\partial E_a/\partial\beta$, which has values of 36.16 to 111.93 (kJ/mol)^2 at 298.15 K and 0.1 MPa based on the fitting. We note that this quantity can be written as

$$\frac{\partial E_a}{\partial \beta} = E_a^2 - \frac{1}{D}\frac{\partial^2 D}{\partial \beta^2}, \tag{25}$$

which indicates that it is determined by the cancellation of two opposing terms that are both significant in magnitude. However, the fits to experimental data clearly indicate that $\partial E_a/\partial\beta$ is positive and the average of all the results is 75.53 (kJ/mol)^2.

The situation is a bit clearer for the pressure dependence of the activation volume. This dependence is weak and found to be (0.83 – 1.82) $\times 10^{-2}$ cm^3/(mol MPa). Note that this derivative and the value of $\Delta V^{\ddagger}(p_0,\beta_0)$ indicate that the activation volume changes in sign as the pressure is increased, but this requires an increase of the pressure by ~ 100 MPa.

Finally, the key elements of the Maxwell relation, eqn (7), are also obtained from the fitting. Namely, $\partial E_a/\partial p$ is negative with values of -5.02 to -9.43 cm^3/mol. This is related to $\beta(\partial\Delta V^{\ddagger}/\partial\beta)$ by $\Delta V^{\ddagger}$, the former of which is thus also negative with values of -3.93 to -8.12 cm^3/mol.

Taken as a whole, differences between the experimental data sets prevent a precise determination of the pressure and temperature dependencies of $D(p,T)$. However, the results do present a consistent semi-quantitative physical picture. The diffusion coefficient and activation energy are quite well determined and in agreement across the different measurements. Greater uncertainty exists in the activation volume and the higher derivatives, but all the data sets agree on the sign of each property. Moreover, the fitting approach illustrates how these fundamental properties of the diffusion coefficient can be determined given sufficiently extensive and accurate measurements.

Lastly, we consider the results of the MD simulations described in Sec. 3. The calculated $D(p,T)$ are shown in Fig. 5 along with the present fit using eqn (24). We note that the fitting is carried out to values of D that do not include a correction for the finite

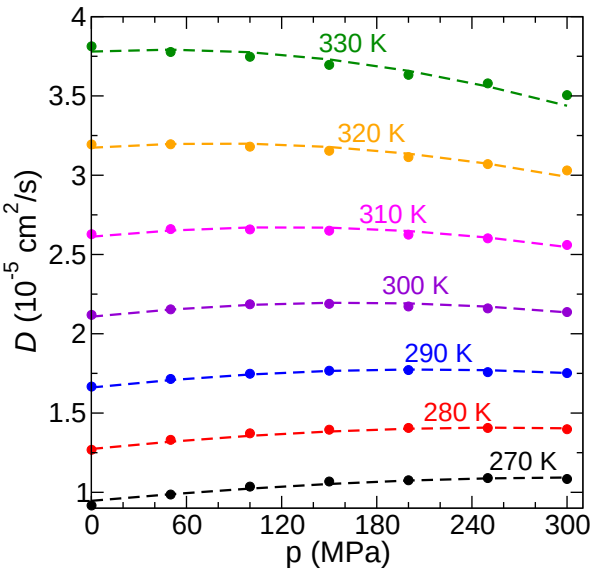

Fig. 5 Comparison of the present simulated $D(p,T)$ values for TIP4P/2005 water compared to its proposed fit to eqn (24). Uncertainties for the simulated diffusion coefficients are smaller than the symbol size.

size of the simulation box based on the viscosity.[54,55] This correction would certainly modify D but should have only a minor effect on the activation energy and volume.[60] Thus, we expect that using the uncorrected diffusion coefficients will have only modest effects on the thermodynamic properties derived from the fitting.

The fit, the parameters for which are given in Table 1, accurately describes the simulation data with average and maximum fit errors comparable to those found for the experimental data sets. The simulation data fitting gives values for the diffusion coefficient, activation energy, and activation volume that are consistent with our earlier calculations in which the latter two are determined directly from simulations at 298.15 K and 0.1 MPa.[36] Further, they are in accord with the results from the experimental data. The values of $\partial E_a/\partial\beta$ and $\partial\Delta V^{\ddagger}/\partial p$ are also within (or close to) the range of experimental results. However, the cross-derivative in β and p, *i.e.*, $\partial E_a/\partial p$ or $\partial\Delta V^{\ddagger}/\partial\beta$, is larger in magnitude (more negative) than that obtained from any of the experimental data sets. It does have the same sign, indicating that the TIP4P/2005 water simulation results are consistent with the qualitative thermodynamic properties of the idealized transition state for diffusion as derived from the experimental measurements. However, the model clearly exhibits an activation energy (volume) that is too sensitive to pressure (temperature).

4.2 Interpretation

A century ago Tolman introduced an alternative, rigorous interpretation of the activation energy.[4,61] The essence of the approach can be simply illustrated by consideration of the cumulative reaction probability, $\mathcal{N}(E,V)$, which is the total probability of reaction at a given total energy E and total volume V.[62] The reaction rate constant at constant pressure and temperature can be obtained from this cumulative reaction probability by appropriate averaging:[35,63]

$$k(p,T) = \frac{1}{2\pi\hbar\Omega_r(p,T)}\int_0^\infty dE\int_0^\infty dV\, e^{-\beta(E+pV)}\mathcal{N}(E,V), \quad (26)$$

where $\Omega_r(p,T)$ is the isothermal-isobaric ensemble partition function of the reactants. It is then straightforward to show that the activation energy, eqn (3), is given by

$$\begin{aligned} E_a &= \frac{\int_0^\infty dE\int_0^\infty dV\, e^{-\beta(E+pV)}(E+pV)\mathcal{N}(E,V)}{\int_0^\infty dE\int_0^\infty dV\, e^{-\beta(E+pV)}\mathcal{N}(E,V)} \\ &+ \frac{1}{\Omega_r}\frac{\partial\Omega_r}{\partial\beta}. \end{aligned} \quad (27)$$

The second term is just equal to the negative of the average reactant enthalpy, $-\langle\mathscr{H}\rangle_r$, while the first term can be simplified by defining the normalized probability of reacting at a given E and V,

$$P_{reacting}(E,V) = \frac{e^{-\beta(E+pV)}\mathcal{N}(E,V)}{\int_0^\infty dE\int_0^\infty dV\, e^{-\beta(E+pV)}\mathcal{N}(E,V)}. \quad (28)$$

Then, the activation energy can be written in an intuitive form as

$$E_a = \langle\mathscr{H}\rangle_{reacting} - \langle\mathscr{H}\rangle_r, \quad (29)$$

where

$$\begin{aligned} \langle\mathscr{H}\rangle_{reacting} &= \int_0^\infty dE\int_0^\infty dV e^{-\beta(E+pV)} \\ &\times (E+pV)P_{reacting}(E,V). \end{aligned} \quad (30)$$

eqn (29) is the isothermal-isobaric ensemble version of Tolman's result,[4] which provides the important interpretation of the activation energy as the average enthalpy of all reacting species minus the average enthalpy of all reactants. This is an alternative to the typical meaning ascribed to E_a as the (approximate) barrier that must be overcome by reactants to react, replacing it instead with the additional energy reacting species have (above the average energy of the reactants) that allows them to overcome the barrier. Note that the latter interpretation enables a rigorous decomposition of the activation energy into different kinetic and potential energy contributions (that help or hinder passage from reactants to products), while the standard barrier interpretation does not.[35,36,64–67]

A completely analogous approach can be used to show that the activation volume in eqn (4) is given by

$$\Delta V^{\ddagger} = \langle V\rangle_{reacting} - \langle V\rangle_r, \quad (31)$$

where

$$\langle V\rangle_{reacting} = \int_0^\infty dE\int_0^\infty dV e^{-\beta(E+pV)}VP_{reacting}(E,V). \quad (32)$$

This provides the Tolman interpretation to the activation volume as the difference in average volume of reacting species minus the average volume of reactants. Note that these volumes include not only the reacting molecules, but any solvent or other species that

rearrange as part of the reaction.[30] In the case of water diffusion, the activation volume can be positive or negative depending on the pressure and temperature, but is negative at 298.15 K and 0.1 MPa (Table 1), indicating that $\langle V\rangle_{reacting} < \langle V\rangle_r$, *i.e.*, the effective transition state for diffusion is more compact than the reactants at ambient conditions.

A key feature of the relationships in eqn (29) and (31) is that the averages over reacting species, $\langle \mathscr{H}\rangle_{reacting}$ and $\langle V\rangle_{reacting}$, include all the effects of transition state recrossing and require no explicit definition of a transition state dividing surface. Instead, they can be viewed as the thermodynamic properties of an idealized transition state dividing surface that exhibits no recrossing.[68] In addition to the obvious advantages this provides, it makes the interpretation readily applicable to timescales that are not obtained directly from rate constants, *e.g.*, diffusion coefficients (*vide infra*), reorientation times, and viscosity.

For the present purposes, eqn (29) provides a simple interpretation of the derivatives of the activation energy itself. Namely, it is easy to see that non-Arrhenius effects are encapsulated in

$$\frac{\partial E_a}{\partial \beta} = -k_B T^2 \left[C_{p,reacting} - C_{p,r}\right], \tag{33}$$

where $C_{p,reacting} = \partial\langle \mathscr{H}\rangle_{reacting}/\partial\beta$ and $C_{p,r} = \partial\langle \mathscr{H}\rangle_r/\partial\beta$ are the constant pressure heat capacities of all species that react and all reactants, respectively. This interpretation of non-Arrhenius behavior that can be derived from Tolman's perspective has been previously recognized.[23] The results for water diffusion given in Table 1 show that for all the measured data sets, $(\partial E_a/\partial\beta) > 0$, which means that $C_{p,r} > C_{p,reacting}$. A molecular-level explanation of this result is currently lacking, but should be an important component of detailed models of water diffusion.

Similarly, the change in activation volume with pressure is given a straightforward interpretation from eqn (31) as

$$\frac{\partial \Delta V^{\ddagger}}{\partial p} = \frac{\partial \langle V\rangle_{reacting}}{\partial p} - \frac{\partial \langle V\rangle_r}{\partial p}. \tag{34}$$

However, these properties are related to the corresponding isothermal compressibilities, *e.g.*,

$$\kappa_{T,reacting} = -\frac{1}{\langle V\rangle_{reacting}} \frac{\partial \langle V\rangle_{reacting}}{\partial p}, \tag{35}$$

for species that successfully react. This gives the derivative of the activation volume with respect to pressure in terms of the difference in isothermal compressibility of reacting species relative to reactants,

$$\frac{\partial \Delta V^{\ddagger}}{\partial p} = -\left[\langle V\rangle_{reacting}\kappa_{T,reacting} - \langle V\rangle_r \kappa_{T,r}\right], \tag{36}$$

in analogy to eqn (33). For water diffusion, we find that $(\partial \Delta V^{\ddagger}/\partial p)$ is relatively small; large pressure increases are required to change the activation volume. This derivative is also positive at ambient conditions, indicating $\langle V\rangle_r \kappa_{T,r} > \langle V\rangle_{reacting}\kappa_{T,reacting}$, however, because $\langle V\rangle_r > \langle V\rangle_{reacting}$, it is not possible to draw an umambiguous conclusion about the relative magnitudes of $\kappa_{T,r}$ and $\kappa_{T,reacting}$.

The pressure dependence of the activation energy and the temperature dependence of the activation volume are connected by the Maxwell relation in eqn (7), which is a dynamical analogy to the Maxwell relation in eqn (20). Namely, we have from eqn (29),

$$\frac{\partial E_a}{\partial p} = \frac{\partial \langle \mathscr{H}\rangle_{reacting}}{\partial p} - \frac{\partial \langle \mathscr{H}\rangle_r}{\partial p}, \tag{37}$$

but using eqn (19) we have,

$$\begin{aligned} \frac{\partial \langle \mathscr{H}\rangle_{reacting}}{\partial p} &= \langle V\rangle_{reacting} + \beta\left(\frac{\partial \langle V\rangle_{reacting}}{\partial \beta}\right)_p, \\ &= \langle V\rangle_{reacting} - T\left(\frac{\partial \langle V\rangle_{reacting}}{\partial T}\right)_p. \end{aligned} \tag{38}$$

The second term can be expressed in terms of the coefficient of thermal expansion,

$$\alpha_{reacting} = \frac{1}{\langle V\rangle_{reacting}}\left(\frac{\partial \langle V\rangle_{reacting}}{\partial T}\right)_p. \tag{39}$$

This gives the β derivative of the activation volume, using eqn (31), as

$$\frac{\partial \Delta V^{\ddagger}}{\partial \beta} = -k_B T^2 [\langle V\rangle_{reacting}\alpha_{reacting} - \langle V\rangle_r \alpha_r] \tag{40}$$

and, the pressure derivative of the activation energy, using eqn (29) as

$$\frac{\partial E_a}{\partial p} = \Delta V^{\ddagger} - T[\langle V\rangle_{reacting}\alpha_{reacting} - \langle V\rangle_r \alpha_r]. \tag{41}$$

In this way, these derivatives are related to the difference in the thermodynamic properties of the reacting and reactant species. From Table 1 we see that $\beta(\partial \Delta V^{\ddagger}/\partial\beta) < 0$ at 298.15 K and 0.1 MPa, so that $\langle V\rangle_{reacting}\alpha_{reacting} > \langle V\rangle_r \alpha_r$. Given that $\langle V\rangle_r > \langle V\rangle_{reacting}$, we can conclude that $\alpha_{reacting} > \alpha_r$.

4.3 Water Shear Viscosity

It is interesting to compare the results obtained from fitting the water self-diffusion coefficient to that for the water shear viscosity, η. The two are naturally linked through the Stokes-Einstein (SE) relation

$$D = \frac{k_B T}{C\pi r \eta}, \tag{42}$$

where r is the hydrodynamic radius of the diffusing particle and C is a constant that is 4 or 6 depending on the diffusion boundary conditions (slip or stick, respectively). The observation and explanation of deviations of water diffusion from SE behavior has attracted significant attention.[7,8,14,17,59,60] The SE relation also implies that the diffusion and viscosity activation energies are related by

$$E_{a,D} = E_{a,\eta} + k_B T, \tag{43}$$

where $E_{a,\eta} = -(\partial \ln \eta^{-1}/\partial\beta)$; this eliminates any uncertainty in evaluating the SE relation that can arise from the choice of the value of C. We have previously used direct calculations of diffusion coefficient and viscosity activation energies to test SE behav-

Table 2 Summary of nonlinear least-squared fits of eqn (24) to experimental measurements of the water shear viscosity, η, as a function of p and T.[7,14,17,19–21,37,38] Values are for $T_0 = 298.15$ K and $p_0 = 0.1$ MPa.

Quantity	Cappi[7,37,38]	Harris & Woolf[19,20]	Singh *et al.*[17]	Jonas *et al.*[14]	Abramson[21]	Units
η	0.896	0.910	0.908	0.865	0.767	mPa s
$E_{a,\eta}$	16.52	16.11	16.81	15.41	13.97	kJ/mol
$\Delta V_\eta^\ddagger$	-0.69	-1.19	-1.73	1.06	2.07	cm^3/mol
$\frac{\partial E_{a,\eta}}{\partial \beta}$	70.49	71.11	86.92	55.69	78.37	$(kJ/mol)^2$
$\frac{\partial \Delta V_\eta^\ddagger}{\partial p}$	1.10	1.15	1.73	0.14	0.0073	10^{-2} cm^3/(mol MPa)
$\frac{\partial E_{a,\eta}}{\partial p}$	-10.72	-3.74	-10.19	-0.36	3.28	cm^3/mol
$\beta \frac{\partial \Delta V_\eta^\ddagger}{\partial \beta}$	-10.03	-2.55	-8.46	-1.42	1.21	cm^3/mol
RMSE	0.0 034	0.021	0.056	0.028	0.081	mPa s
χ^2	0.31[a]	1.17[a]	1.01	1.22[b]	1.62[c]	
Avg. Fit Error	0.25	0.92	1.45	1.94	3.85	%
Max. Fit Error	0.84	3.90	5.92	7.07	12.28	%

[a] Assumes 1% error for all data points.
[b] Assumes 2% error for all data points.
[c] Assumes 3% error for all data points.

ior through eqn (43).[60]

An extended comparison involving a fuller set of activation parameters can be made through the fitting approach proposed here, in which we write

$$\begin{aligned} \ln \frac{\eta^{-1}(p,\beta)}{\eta^{-1}(p_0,\beta_0)} &= -E_{a,\eta,0}\Delta\beta - \beta\Delta V^\ddagger_{\eta,0}\Delta p \\ &- \frac{1}{2}\left.\frac{\partial E_{a,\eta}}{\partial \beta}\right|_0 \Delta\beta^2 - \frac{\beta_0}{2}\left.\frac{\partial \Delta V_\eta^\ddagger}{\partial p}\right|_0 \Delta p^2 \\ &- \beta_0 \left.\frac{\partial \Delta V_\eta^\ddagger}{\partial \beta}\right|_0 \Delta p \Delta\beta, \end{aligned} \quad (44)$$

in analogy to eqn (24) for the diffusion coefficient. We have applied this to five data sets from experimental measurements reported in the literature and the parameters obtained from the fitting are given in Table 2.

The five viscosity data sets can be roughly divided into three[7,17,19,20,37,38] obtained at pressures < 400 MPa and two including measurements at substantially higher pressures.[14,21] We first consider the former group, the results for which are given in the first three data columns of Table 2 and plotted in Figs. 6, 7, and 8. The fits to eqn (44) are in excellent agreement with the data in all three cases, with average errors of less than 1.5% and maximum errors of $< 6\%$. The largest deviations occur at low temperatures.

The activation parameters from the three lower-pressure fits are in excellent qualitative and reasonable quantitative agreement. The activation energy at 298.15 K and 0.1 MPa is found to be in the range $16.11 - 16.81$ kJ/mol, in good agreement with

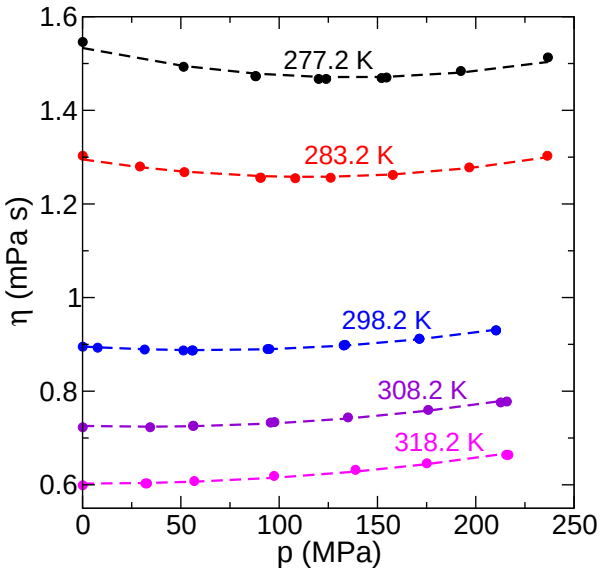

Fig. 6 Comparison of measured $\eta(p,T)$ (circles) from Cappi (Refs. 7,37, 38) compared to its fit (dashed lines) to eqn (44).

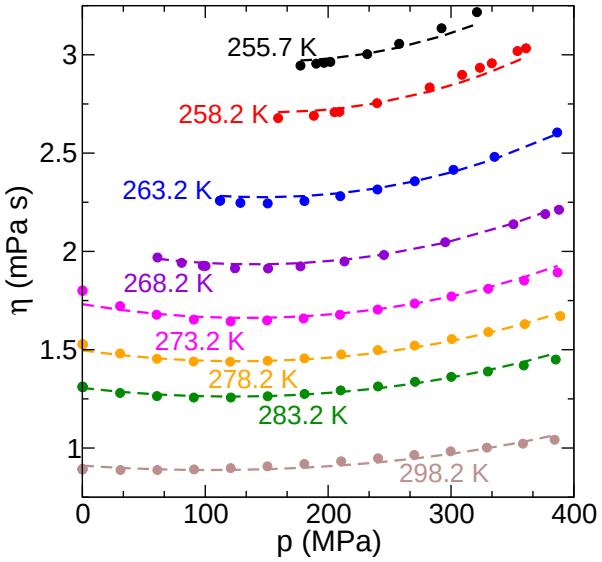

Fig. 7 Comparison of measured $\eta(p,T)$ (circles) from Harris and Woolf (Refs. 19 and 20) compared to its fit (dashed lines) to eqn (44).

the value obtained by Woolf.[7] These results are too high compared to the Stokes-Einstein prediction, eqn (43), based on the diffusion coefficient activation energies in Table 1, which would give $E_{a,\eta} = 14.65 - 15.95$ kJ/mol. This is consistent with our previous comparison of the activation energies from MD simulations, which found deviations from the Stokes-Einstein description for water diffusion.[60] The remaining activation parameters are in general agreement with those obtained for D given the variations between the data sets. The viscosity activation volume is negative and on the same order as that for D (approximately -1 cm^3/mol). Similarly, the temperature dependence of the activation energy, $\partial E_{a,\eta}/\partial\beta$ is between $70-87$ kJ/mol in accord with the diffusion results. Both D and η also have similar pressure dependence of the activation volume, with $\partial\Delta V_\eta^\ddagger/\partial p$ on the order of $1.1 - 1.7\times10^{-2}$ cm^3/(mol MPa). Finally, $\partial E_{a,\eta}/\partial p$ and $\partial\Delta V_\eta^\ddagger/\partial\beta$ vary in magnitude between data sets for both D and η, but are uniformly negative and of similar absolute values. Overall, these similarities indicate the common process of the exchange of hydrogen-bond partners that underlies both diffusion and viscosity,[22,69] and point to the need for more precise and detailed characterizations of the subtle mechanistic differences between each property and the exchange rate constant.

The other two viscosity data sets, those of Jonas *et al.*[14] and Abramson,[21] are concentrated on significantly higher pressures, extending to ~ 900 and nearly 5700 MPa, respectively. The fit parameters using eqn (44) are given in Table 2 and the results are plotted in Figs. 9 and 10. The fits are not as accurate as for the lower pressure results in Figs. 6-8, but are in quite reasonable agreement with the measured data across the range of p and T, with average errors of less than 4%. However, the resulting activation parameters change significantly compared to the lower pressure results. In particular, the activation energy is re-

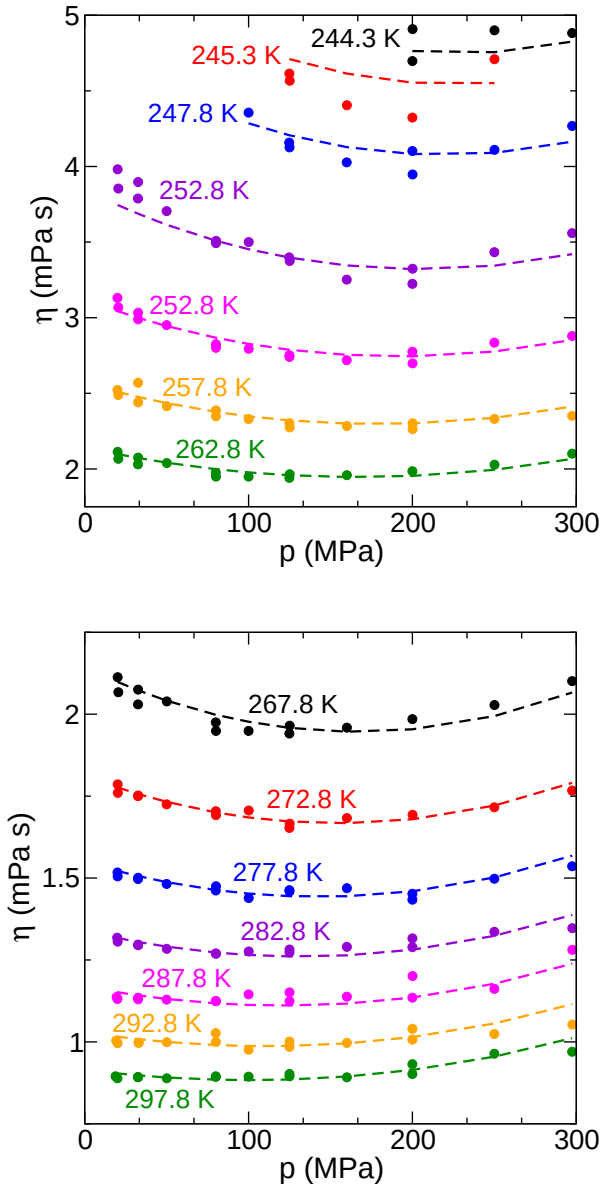

Fig. 8 Comparison of measured $\eta(p,T)$ (circles) from Singh *et al.* (Ref. 17) compared to its fit (dashed lines) to eqn (44) at low (top panel) and high (bottom panel) temperatures.

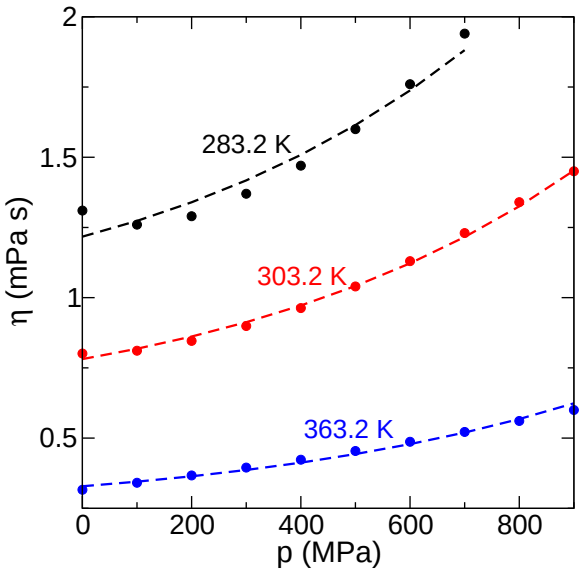

Fig. 9 Comparison of measured $\eta(p,T)$ (circles) from Jonas *et al.* (Ref. 14) compared to its fit (dashed lines) to eqn (44).

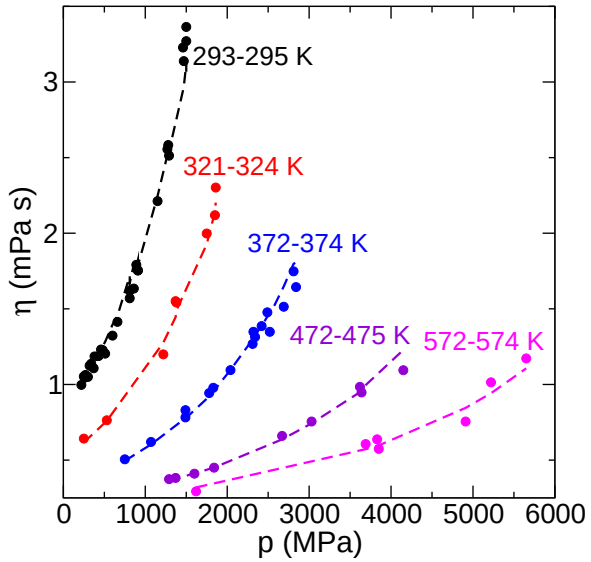

Fig. 10 Comparison of measured $\eta(p,T)$ (circles) from Abramson (Ref. 21) compared to its fit (dashed lines) to eqn (44).

duced and the activation volume becomes positive; both changes appear to be correlated with the increase in pressures included in the data set. Further, $\partial \Delta V_\eta^\ddagger / \partial p$ decreases substantially and $\partial E_{a,\eta}/\partial p$ and $\partial \Delta V_\eta^\ddagger / \partial \beta$ increase modestly. The non-Arrhenius measure, $\partial E_{a,\eta}/\partial \beta$ is, however, largely unchanged. The results indicate that, while the fitting approach represented in eqn (44), is flexible enough to describe data sets over a wide range of p and T, the activation parameters at a particular p_0 and β_0 are best obtained from measurements (or simulations) that are focused on nearby pressures and temperatures.

5 Conclusions

We have introduced a Maxwell relation for a reaction rate constant, or other dynamical timescale, that is completely analogous to the corresponding thermodynamic relationship. In particular, this dynamical Maxwell relation connects the higher-order temperature and pressure dependencies of the rate constant. Using fluctuation theory we show how these are fundamentally related to each other through the correlation of energy and volume fluctuations with reactivity.

The Maxwell relation is used as the basis for proposing a physically-motivated mathematical description of a rate constant as a function of temperature and pressure. A key advantage of such an approach is that the (six) fitting parameters are each meaningful quantities, *e.g.*, the activation energy, activation volume, and their derivatives with respect to pressure and temperature.

We have illustrated this description by using it to fit experimentally measured values of the liquid water self-diffusion coefficient and shear viscosity. The diffusion coefficients reported in several NMR and diaphragm cell studies[7–11] as well as simulation results for the TIP4P/2005 water model were first considered using this Maxwell relation. Five experimental viscosity data sets were also fit.[7,14,17,19–21,37,38] The fits are highly accurate and, more importantly, give quantitative insight into the activation parameters and their pressure and temperature dependence. Specifically, the experimental fits yield values at 298.15 K and 0.1 MPa for the diffusion coefficient, $(2.2-2.29)\times 10^{-5}$ cm^2/s, and the activation energy, $17.1-18.4$ kJ/mol, that are in good quantitative agreement across the data sets considered. The quantitative values of the other quantities vary more strongly between the different measurements, but they are all in qualitative agreement. Namely, the activation volume is negative, consistent with the notion that increasing pressure from ambient conditions disrupts the hydrogen-bonding network thereby accelerating water diffusion. Non-Arrhenius effects are prominent, with the activation energy increasing as temperature is lowered. In contrast, the activation energy decreases with increasing pressure, further indicative of pressure-induced disruption of the water hydrogen-bonding structure; this further requires, through the dynamical Maxwell relation, that the activation volume decrease as the temperature is lowered.

An interesting comparison of the viscosity and diffusion coefficient activation parameters is provided by the fitting (limiting ourselves to the lower pressure viscosity data). Notably, the viscosity activation energies are higher than is predicted from the

diffusion coefficient results assuming Stokes-Einstein behavior.[60] Beyond this, however, the activation parameters are in reasonable accord, within the variations in results between the data sets. The activation volumes and their pressure dependence are quantitatively similar for D and η. Similarly, the activation energy temperature and pressure dependences have the same sign and magnitude for the viscosity and diffusion coefficient as well. In this way, these fits provide useful insight into the similarities and differences in the thermodynamic properties of the hypothetical perfect transition states for water diffusion and shear viscosity.

These applications of the fitting approach illustrate how measured dynamical timescales as a function of pressure and temperature can be described, and fit, in a physically meaningful way. This should be a useful alternative method for fitting such experimental data to the typical approaches based on empirical formulas. It also will provide closer connections to, and benchmarks for, theoretical calculations by determining the values of activation parameters.

Conflicts of interest

There are no conflicts to declare.

Acknowledgments

The authors would like to thank Professor Brian B. Laird for many useful discussions. This work was supported by the National Science Foundation under Grant Nos. CHE-1800559 and CHE-2102656. This material is based on the work supported by the National Science Foundation Graduate Research Fellowship under Grant Nos. 1540502 and 1451148 as well as the National Science Graduate Research Opportunities Worldwide Program (Z.A.P.). A.K.B. gratefully acknowledges support from a University of Kansas Dean's Doctoral Fellowship. The calculations were performed at the University of Kansas Center for Research Computing (CRC), including including the BigJay cluster resource funded through NSF Grant MRI-2117449.

References

1 D. A. McQuarrie and J. D. Simon, *Physical Chemistry: A Molecular Approach*, University Science Books, Sausalito, CA, 1997.
2 A. Arrhenius, *Z. Physik. Chem.*, 1889, **4**, 226–248.
3 K. J. Laidler, *J. Chem. Educ.*, 1984, **61**, 494–498.
4 R. C. Tolman, *J. Am. Chem. Soc.*, 1920, **42**, 2506–2528.
5 R. van Eldik, T. Asano and W. J. le Noble, *Chem. Rev.*, 1989, **89**, 549–688.
6 A. Drljaca, C. D. Hubbard, R. van Eldik, T. Asano, M. V. Basilevsky and W. J. le Noble, *Chem. Rev.*, 1998, **98**, 2167–2290.
7 L. A. Woolf, *J. Chem. Soc., Faraday Trans. 1*, 1975, **71**, 784–796.
8 K. Krynicki, C. D. Green and D. W. Sawyer, *Faraday Discuss. Chem. Soc.*, 1978, **66**, 199–208.
9 K. R. Harris and L. A. Woolf, *J. Chem. Soc., Faraday Trans. 1*, 1980, **76**, 377–379.
10 K. R. Harris and P. J. Newitt, *J. Chem. Eng. Data*, 1997, **42**, 346–348.
11 F. X. Prielmeier, E. W. Lang, R. J. Speedy and H. D. Lüdemann, *Ber. Bunsenges. Phys. Chem.*, 1988, **92**, 1111–1117.
12 Z. A. Piskulich and W. H. Thompson, *J. Chem. Phys.*, 2020, **152**, 074505.
13 H. Weingärtner, *Z. Phys. Chem.*, 1982, **132**, 129–149.
14 J. Jonas, T. DeFries and D. J. Wilbur, *J. Chem. Phys.*, 1976, **65**, 582–588.
15 T. DeFries and J. Jonas, *J. Chem. Phys.*, 1977, **66**, 5393–5399.
16 F. X. Prielmeier, E. W. Lang, R. J. Speedy and H. D. Lüdemann, *Phys. Rev. Lett.*, 1987, **59**, 1128–1131.
17 L. P. Singh, B. Issenmann and F. Caupin, *Proc. Natl. Acad. Sci.*, 2017, **114**, 4312–4317.
18 C. H. Cho, J. Urquidi, S. Singh and G. W. Robinson, *J. Phys. Chem. B*, 1999, **103**, 1991–1994.
19 K. R. Harris and L. A. Woolf, *J. Chem. Eng. Data*, 2004, **49**, 1064–1069.
20 K. R. Harris and L. A. Woolf, *J. Chem. Eng. Data*, 2004, **49**, 1851.
21 E. H. Abramson, *Phys. Rev. E*, 2007, **76**, 051203.
22 Z. A. Piskulich, D. Laage and W. H. Thompson, *J. Phys. Chem. A*, 2021, **125**, 9941–9952.
23 D. G. Truhlar and A. Kohen, *Proc. Natl. Acad. Sci.*, 2001, **98**, 848–851.
24 M. J. Pilling and P. W. Seakins, *Reaction Kinetics*, Oxford, New York, 1995.
25 A. Drljaca, C. D. Hubbard, R. Van Eldik, T. Asano, M. V. Basilevsky and W. J. Le Noble, *Chem. Rev.*, 1998, **98**, 2167–2289.
26 D. Spångberg, M. Wojcik and K. Hermansson, *Chem. Phys. Lett.*, 1997, **276**, 114–121.
27 K. Bagchi, S. Balasubramanian and M. L. Klein, *J. Chem. Phys.*, 1997, **107**, 8561–8567.
28 J. R. Rustad and A. G. Stack, *J. Am. Chem. Soc.*, 2006, **128**, 14778–14779.
29 H. V. Annapureddy and L. X. Dang, *J. Phys. Chem. B*, 2014, **118**, 7886–7891.
30 B. M. Ladanyi and J. T. Hynes, *J. Am. Chem. Soc.*, 1986, **108**, 585–593.
31 H. Kelm and D. A. Palmer, in *High Pressure Chemistry*, ed. H. Kelm, D. Reidel, Dordrecht, Holland, 1978, pp. 281–309.
32 H. D. Brauer and H. Kelm, *Zeitschrift fur Phys. Chemie*, 1972, **79**, 96–102.
33 O. O. Mesele and W. H. Thompson, *J. Chem. Phys.*, 2016, **145**, 134107.
34 Z. A. Piskulich, O. O. Mesele and W. H. Thompson, *J. Chem. Phys.*, 2018, **148**, 134105.
35 Z. A. Piskulich, O. O. Mesele and W. H. Thompson, *J. Phys. Chem. A*, 2019, **123**, 7185–7194.
36 Z. A. Piskulich and W. H. Thompson, *J. Chem. Theory Comput.*, 2021, **17**, 2659–2671.
37 J. B. Cappi, *Ph.D. thesis*, 1964.
38 K. E. Bett and J. B. Cappi, *Nature*, 1965, **207**, 620–621.
39 C. A. Angell, E. D. Finch, L. A. Woolf and P. Bach, *J. Chem. Phys.*, 1976, **65**, 3063–3074.

40 J. L. F. Abascal and C. Vega, *J. Chem. Phys.*, 2005, **123**, 234505.

41 A. P. Thompson, H. M. Aktulga, R. Berger, D. S. Bolintineanu, W. M. Brown, P. S. Crozier, P. J. in 't Veld, A. Kohlmeyer, S. G. Moore, T. D. Nguyen, R. Shan, M. J. Stevens, J. Tranchida, C. Trott and S. J. Plimpton, *Comp. Phys. Comm.*, 2022, **271**, 108171.

42 S. Nosé, *Mol. Phys.*, 1984, **52**, 255–268.

43 W. G. Hoover, *Phys. Rev. A*, 1985, **31**, 1695–1697.

44 T. Darden, D. York and L. Pedersen, *J. Chem. Phys.*, 1993, **98**, 10089–10092.

45 E. L. Pollock and J. Glosli, *Comput. Phys. Comm.*, 1995, **95**, 93–110.

46 D. P. Shoemaker, C. W. Garland and J. W. Nibler, *Experiments in Physical Chemistry*, McGraw-Hill, New York, 1989.

47 V. Aquilanti, N. D. Coutinho and V. H. Carvalho-Silva, *Philos. Trans. R. Soc. A*, 2017, **375**, 20160201.

48 V. H. Carvalho-Silva, N. D. Coutinho and V. Aquilanti, *Front. Chem.*, 2019, **7**, 380.

49 P. W. Bridgman, *Proc. Am. Acad. Arts Sci.*, 1927, **62**, 207–226.

50 Y. Xu, N. G. Petrik, R. S. Smith, B. D. Kay and G. A. Kimmel, *Proc. Natl. Acad. Sci.*, 2016, **113**, 14921–14925.

51 N. J. Hestand and J. L. Skinner, *J. Chem. Phys.*, 2018, **149**, 140901.

52 P. Gallo, K. Amann-Winkel, C. A. Angell, M. A. Anisimov, F. Caupin, C. Chakravarty, E. Lascaris, T. Loerting, A. Z. Panagiotopoulos, J. Russo, J. A. Sellberg, H. E. Stanley, H. Tanaka, C. Vega, L. Xu and L. G. M. Pettersson, *Chem. Rev.*, 2016, **116**, 7463–7500.

53 R. Mills, *J. Phys. Chem.*, 1973, **77**, 685–688.

54 B. Dunweg and K. Kremer, *J. Chem. Phys.*, 1993, **99**, 6983–6997.

55 I.-C. Yeh and G. Hummer, *J. Phys. Chem. B*, 2004, **108**, 15873–15879.

56 K. R. Harris, *Phys. Chem. Chem. Phys.*, 2002, **4**, 5841–5845.

57 J. C. Palmer, F. Martelli, Y. Liu, R. Car, A. Z. Panagiotopoulos and P. G. Debenedetti, *Nature*, 2014, **510**, 385–388.

58 J. C. Palmer, P. H. Poole, F. Sciortino and P. G. Debenedetti, *Chem. Rev.*, 2018, **118**, 9129–9151.

59 P. Montero De Hijes, E. Sanz, L. Joly, C. Valeriani and F. Caupin, *J. Chem. Phys.*, 2018, **149**, 094503.

60 C. H. Mendis, Z. A. Piskulich and W. H. Thompson, *J. Phys. Chem. B*, 2019, **123**, 5857–5865.

61 D. G. Truhlar, *J. Chem. Ed.*, 1978, **55**, 309–311.

62 W. H. Miller, S. D. Schwartz and J. W. Tromp, *J. Chem. Phys.*, 1983, **79**, 4889–4898.

63 R. D. Levine and R. B. Bernstein, *Molecular Reaction Dynamics and Chemical Reactivity*, Oxford University Press, New York, 1987.

64 N. C. Blais, D. G. Truhlar and B. C. Garrett, *J. Phys. Chem.*, 1981, **85**, 1094–1096.

65 N. C. Blais, D. G. Truhlar and B. C. Garrett, *J. Chem. Phys.*, 1982, **76**, 2768–2770.

66 H. Rafatijo and D. L. Thompson, *J. Chem. Phys.*, 2017, **147**, 224111.

67 Z. A. Piskulich, O. O. Mesele and W. H. Thompson, *J. Chem. Phys.*, 2017, **147**, 134103.

68 Such a non-recrossing dividing surface is presumably a function of both coordinates and momenta.

69 A. Gomez, Z. A. Piskulich, W. H. Thompson and D. Laage, *J. Phys. Chem. Lett.*, 2022, **13**, 4660–4666.